Effect of Solvent Evaporation Time and Casting Thickness on the Separation Performance of Cellulose Acetate Butyrate Blend Membrane

Darvin Manimaran[a], Zeinab Abbas Jawad[a]* & Chew Thiam Leng[b,c]

[a]Department of Chemical Engineering, Faculty of Engineering and Science, Curtin University Malaysia, CDT 250, 98009 Miri, Sarawak, Malaysia
[b]Department of Chemical Engineering, Faculty of Engineering, Universiti Teknologi PETRONAS, 32610 Seri Iskandar, Perak, Malaysia
[c]CO2 Research Centre (CO2RES), Institute of Contaminant Management, Universiti Teknologi PETRONAS, 32610 Seri Iskandar, Perak, Malaysia

ABSTRACT

Global warming and climate change due to greenhouse gases (GHGs) emission, mostly carbon dioxide (CO_2), have induced global efforts to minimize the concentration of atmospheric CO_2. To reduce the effects of this problem, membrane technology is selected for the separation of CO_2 due to the energy efficiency and economic advantages exhibited. In this study, the chosen polymeric material, cellulose acetate butyrate (CAB) is optimized using a wet phase inversion method with various molecular weight and different casting conditions due to its outstanding film-forming specifications and capabilities of fabricating a defect-free layer of neat membrane. The membrane was synthesized by blending three different molecular weights (Mn) of 12,000, 30,000 and 70,000 at different casting thickness, 150 μm to 300 μm and solvent evaporation time of 3.5 to 5 min. The results of these predominant parameters were then utilized to determine a high performance CAB membrane suitable for an enhanced CO_2/Nitrogen (N_2) separation. Eventually, a high separation performance CAB membrane was successfully synthesized with a CO_2/N_2 selectivity of 1.5819 ± 0.0775 when the solvent evaporation time and casting thickness was optimized at 4.5 min and 300 μm, respectively. Through this study, an improved understanding between membrane casting conditions and membrane performance has been achieved, for future development and progress.

Keywords: Cellulose acetate butyrate, casting thickness, solvent evaporation time, polymer molecular weight, CO_2/N_2 separation

1.0 INTRODUCTION

The continued development of climate change due to greenhouse gasses (GHGs) emission, mostly carbon dioxide (CO_2) has become a severe concern globally [1]. Therefore, well-constructed solutions and adaptation strategies, if adopted quickly, could significantly reduce the effects of climate change. Membrane gas separation technology can be one of the approaches examined to address the increased levels of atmospheric CO_2 [2].

Membrane separation is extensively investigated, as it has numerous advantages [3] compared to conventional processes, such as low capital and operating cost, lower energy requirements, basic process configuration as well as minimized

footprint [4]. Furthermore, the performance of polymeric membrane, the most commonly studied CO_2 membrane technology, is defined by the relationship between selectivity and permeability, which is also the main challenge in the permeation technology [1].

The polymeric membrane fabrication is controlled by a variation of parameters that would ultimately affect the permeability and selectivity of the membrane. Casting thickness is one of the important parameter as it influences the membrane morphology and separation performance which would directly influence the efficiency of the gas separation [5]. According to Jawad *et al.* (2015), a thin membrane layer is essential to achieve a high efficiency [6]. This is because, the gas permeability of the membrane increases as the thickness layer decreases [7].

Besides that, solvent evaporation time is also another influential parameter as it affects the formation of undesired macrovoids [8]. According to Holda *et al.* [9], the membrane skin layer decreases with an increased evaporation time leading to morphologies with less macrovoid in the substructure. This allows gas to pass through the membrane structure at a faster rate. Hence, according to Lee *et al.* [2], the dominant specification for solvent evaporation time was 5 minutes as a better selectivity and consistent permeances result were observed for cellulose acetate butyrate (CAB) with molecular weight (Mn) of 70000.

Thus, the aim of this research project is to produce a high efficiency performance of CAB polymer matrix for the improvement of CO_2/N_2 separation. Up to date, many works have been conducted, aimed at enhancing membrane performance for numerous membrane separation processes. However, there is no research study combined the effect of membrane casting thickness and solvent evaporation time, together with the molecular weight of CAB of 12,000, 30,000 and 70,000 at a ratio of 1:2:2 for gas separation. This is because Mn of polymeric membranes has a momentous influence on the rheology of the polymer solution which manipulates the structure and the performance of the final membranes [10]. Therefore, by synthesizing a membrane by blending three different molecular weights of CAB, the membrane surface hydrophilicity can be improved because of the presence of the extra hydroxyl ($O-H$) and carbonyl groups ($C\equiv O$) originating from the CAB of each Mn [11]. In addition, these highly polar functional groups, $C\equiv O$ and $O-H$, can react with the non-polar CO_2 gas [12]. Hence, enhancing the CO_2 permeability and selectivity of the CAB membrane [13]. Therefore, this research study is believed to further improve the membrane design for gas separation

2.0 METHODS

2.1 Materials

The cellulose acetate butyrate (CAB) with acetyl content of 12%-15% and polymer molecular weights (Mn) of 12,000, 30,000, and 70,000 was purchased from Sigma-Aldrich (Malaysia) for membrane fabrication. The solvent chloroform (99.7%) was purchased from Merck (Malaysia). The hexane (99.8%) and isopropyl alcohol (99.6%) were supplied by Merck (Malaysia) for membrane drying. Purified carbon dioxide (CO_2) and nitrogen (N_2) were acquired from Linde EOX Sdn Bhd (Malaysia).

Table 1 The composition of membrane fabricated at different casting thickness

CAB Polymer				Solvent (Chloroform)		Casting thickness (μm)	Sample Description
Total (wt%)	Molecular Weight, Mn (g)						
	12,000	30,000	75,000	(wt%)	(ml)		
4	0.8	1.6	1.6	96	64	150	M5
4	0.8	1.6	1.6	96	64	250	M6
4	0.8	1.6	1.6	96	64	300	M7

Table 2 The composition of membrane fabricated at different solvent evaporation time

| CAB Polymer				Solvent (Chloroform)		Solvent Evaporation Time (min)	Sample Description
Total (wt%)	Molecular Weight, Mn (g)						
	12,000	30,000	75,000	(wt%)	(ml)		
4	0.8	1.6	1.6	96	64	3.5	M1
4	0.8	1.6	1.6	96	64	4	M2
4	0.8	1.6	1.6	96	64	4.5	M3
4	0.8	1.6	1.6	96	64	5	M4

2.2 Fabrication of CAB Membrane

Wet phase inversion method was used for the fabrication process of CAB. Phase inversion can be expressed as a demixing procedure whereby the initially homogenous polymer solution was transformed in a controlled manner from a liquid to solid state [14]. The experiment was initiated by preparing a solution consisting of 4 wt% of CAB and 96 wt% of chloroform [2]. The prepared solution was then stirred for 24 hrs before being sonicated for 20 min. The sonication procedure is essential to establish the surface of the neat membrane by eliminating the bubbles in the solution [15]. The next step was casting the membrane with a casting thickness of 150 μm using a casting machine. This is followed by the solvent evaporation for 4.5 minutes at room temperature.

To phase out the residual solvent, the membrane was immersed in a distilled water at a temperature of 22 ˚C for 24 hrs. Later, the fabricated membrane was immersed in isopropyl alcohol and then n-hexane accordingly for 1 hr each. This step was performed to dry the membrane formed. Finally, to eliminate all the excess solvents, the fabricated membrane, was heated in an oven at a temperature of 70 ˚C for 24 hrs. All the mentioned steps were performed respectively for CABs with different molecular weight distribution ranging from Mn 12,000 to Mn 70,000.

2.3 Effect of Casting Thickness

In this study, the membrane was fabricated at different casting thickness ranging from 150 μm to 300 μm with a constant solvent evaporation time of
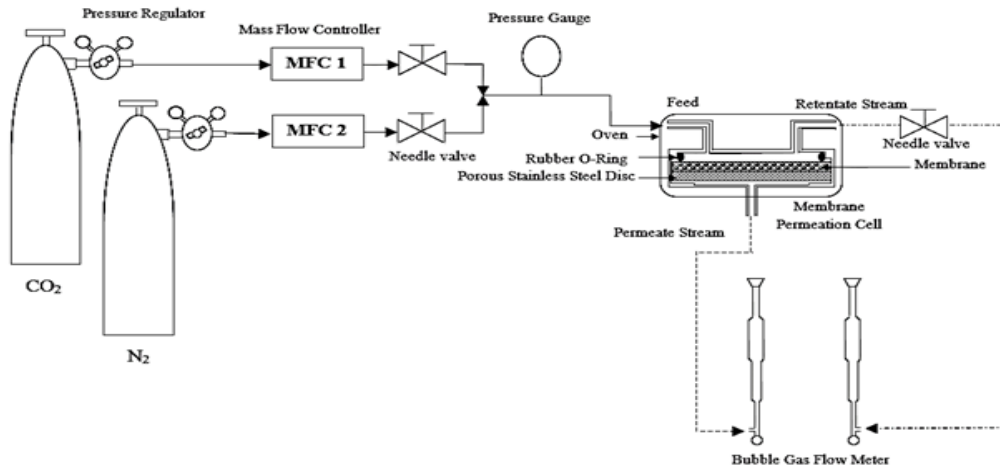
Figure 1 Illustrative diagram of the experimental set-up [2]

4.5 min. The composition of the membrane fabrication is exhibited in Table 1.

2.4 Effect of Solvent Evaporation Time

In this study, the membrane was fabricated at different solvent evaporation time ranging from 3.5 to 5 minutes with a constant membrane thickness of 250 μm. The composition of the membrane fabrication is exhibited in Table 2.

2.5 Gas Permeation Test

Purified CO_2 and N_2 at room temperature was utilized for the gas permeation test. For each single gas permeation test (CO_2 or N_2), the flow rate of the gas was set to release from a compressed gas cylinder tank at a rate of 100ml/min employing a mass flow controller (Aalborg AFC 26, USA). As shown in Figure 1, the mass flow controller was linked to a two-channel digital set point/readout unit (Aalborg 0-200 ml/min, USA). Throughout the experimental investigation, the selected gas was fed into the stainless-steel membrane cell at a pressure ranging from 1-2 bar. To ensure reliable and accurate results, several precautionary measures were

established prior to the membrane testing. First, N_2 gas was streamed through the set up for 10 minutes, to remove any impurity gas within the pipes. This procedure was conducted to prevent leakage and guarantee no feed gas outbreak from the pipes. Next, the synthesized membrane was shaped into a round disc with an approximate diameter of 7.065 cm^2 before being placed in the firmly covered membrane permeation cell. Then, the flowrate of the permeate and retentate was studied individually utilizing the volume displacement method, aided by a soap bubble flow meter [2].

2.6 Gas Separation Performance

The gas permeation and separation performance, was obtained using the following equations and calculations:

Flux of the gas sample, N_i was calculated by the following equation:

$$N_i = \frac{mol\ of\ component\ gas\ A\ permeate\ through\ membrane}{tA_m}$$

where N_i = Flux of gas, mol/m^2.s, A_m = Area, m^2, t = time, s and i = Refer to the gas CO_2 or N_2

Permeability of the membrane, P_i was obtained by the following equation:

$$P_i = \frac{N_i}{\Delta P_i}$$

where P_i = Permeability of membrane, mol/m^2. s. Pa and ΔP_i = Pressure difference across the membrane, Pa.

Ratio of permeability, α_{ij} of CO_2/N_2 was calculated by the following equation:

$$\alpha_{ij} = \frac{P_i}{P_j} = \frac{P_i/l}{P_j/l}$$

2.7 Characterization of Membrane

Scanning Electron Microscope (SEM) and Attenuated Total Reflectance Fourier transform infrared spectroscopy (ATR-FTIR) were used for the characterization of the synthesized membrane.

2.7.1 Scanning Electron Microscope (SEM)

A scanning electron microscope is a highly versatile electron beam instrument that can produce images over 100 times more magnified than commercial optical microscopes. It scans a focused electron beam over a surface to form an image. The electron in the beam interacts with the sample, generating various signals that can be used to acquire information about the surface topography and composition [16]. For this study, a scanning electron microscope (Hitachi TM3000, Japan) was used to establish the membrane surface morphology and cross-sectional structure.

   To carry out SEM characterization, the membrane samples was first cut into small pieces before freezing it in a cryogenic freezer with a petri dish at -80 ˚C for 24 hours. This step was carried out to ensure the membrane structure is consistent and not deformed. Next, the samples were coated with platinum before being observed under the microscope to stop

the accumulation of static charges at the specimen.

Equation 2

2.7.2 Attenuated Total Reflectance Fourier Transform Infrared Spectroscopy (ATR-FTIR)

Attenuated Total Reflectance Fourier transform infrared (ATR-FTIR) spectroscopy is a type of spectroscopy where infrared light is introduced into a prism at an angle beyond the critical angle for internal reflection. This allows the measurement of depth profiles for thin layers and the orientation of molecules adsorbed on the surface [17]. For this study, the ATR-FTIR was used to identify and understand the membrane structure. This method normally does not require any sample preparation.

Equation 3

   Hence, the samples were tested using a Thermo Scientific Fourier transform infrared spectrometer (Nicolet iS10, USA) over the wavenumber range of 425-4000 cm^{-1}. Each spectrum was established from 32 scans at 4 cm^{-1} with a resolution of 45 ˚ incident angle with the help of a diamond crystal.

3.0 RESULTS AND DISCUSSION

3.1 Effect of Casting Thickness

3.1.1 Membrane Characterization

SEM analysis had been carried out to study the membrane morphology and membrane thickness. Figure 2 demonstrates the surface morphology and cross-sectional thickness for the CAB membranes fabricated at different casting thickness of 150 μm (M5), 250 μm (M6) and 300 μm (M7), respectively. Based on Figure 2 (a, c and e), the membrane surface is rough for all casting thickness. In addition, the formation of nodules reduced with

increase the casting thickness of the membrane. This is as a results of the low evaporation rate at high casting thickness Therefore, the nodular structures can aggregate to form less structures [18]. Besides that, according to Figure 2 (b, d and f), when the casting thickness increased from 150 μm (M5) to 300 μm (M7), the membrane thickness also increased from 4.852 ± 0.654 μm to 28.4455 ± 1.314 μm. This is due to the slower polymer deposition speed as more layers were involved in the membrane formation when the membrane was fabricated with a thicker casting thickness. Additionally, the kinetic of phase separation would also be delayed, enabling the combination of polymer-lean domains which are positioned below the membrane-air interface. Hence, forming a thicker membrane as the casting thickness increases [19].
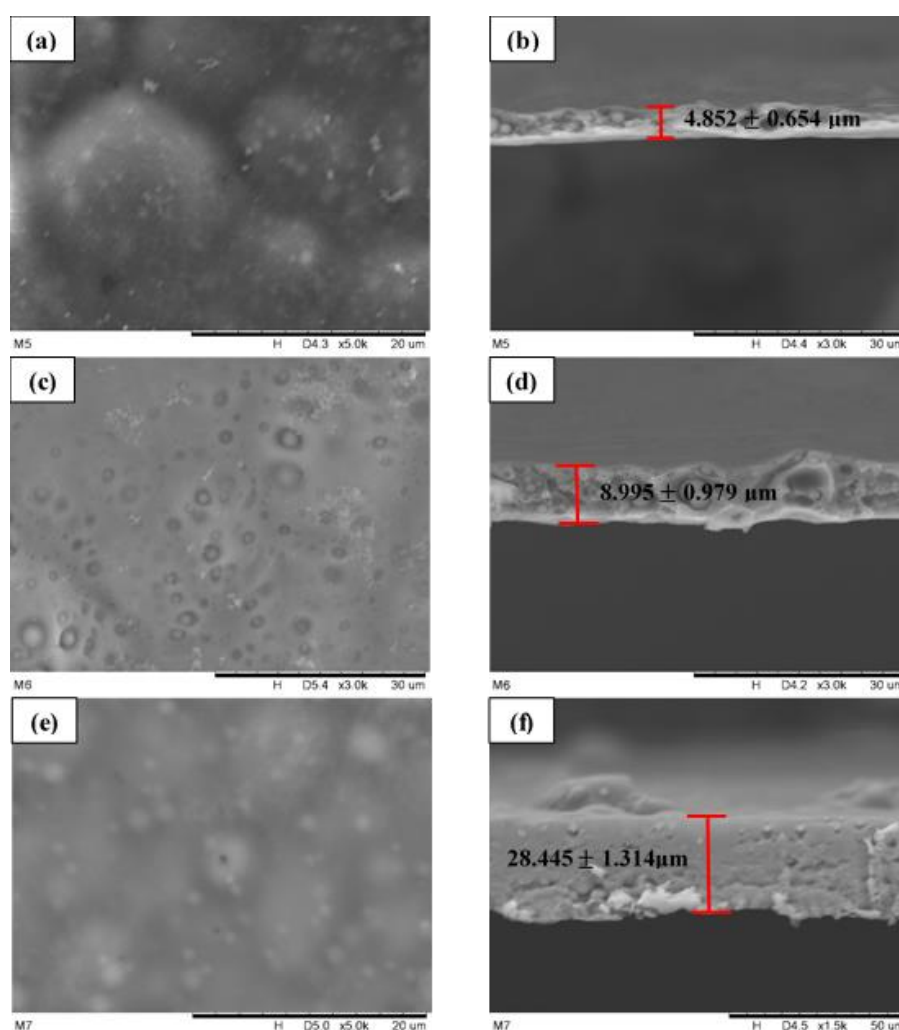
Figure 2 SEM micrographs of membrane surface (left) and cross-section (right) structure synthesized by using 4 wt% of CAB Polymer concentration made up by blending three different molecular weights (Mn) of 12,000, 30,000 and 70,000 at a ratio of 1:2:2, solvent evaporation time of 4.5 min, and solvent exchange drying time of 1 hour for 2-isopropyl alcohol and n-hexane each, with different casting thickness of (a-b) 150 μm (M5), (c-d) 250 μm (M6), and (e-f) 300 μm (M7)
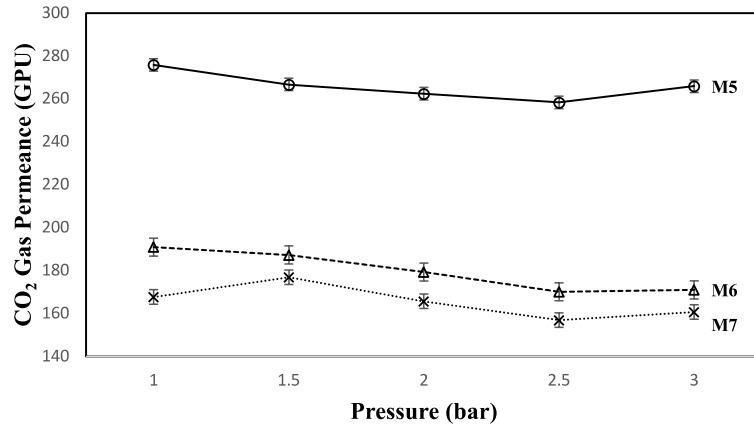
Figure 3 CO_2 Permeance for CAB membrane fabricated with different casting thickness of 150 μm (M5), 250 μm (M6), and 300 μm (M7) with solvent evaporation time of 4.5 min, polymer concentration of 4 wt% made up by blending three different molecular weights (Mn) of 12,000, 30,000 and 70,000 at a ratio of 1:2:2, and solvent exchange drying time of 1 hour each for 2-isopropyl alcohol and n-hexane, respectively
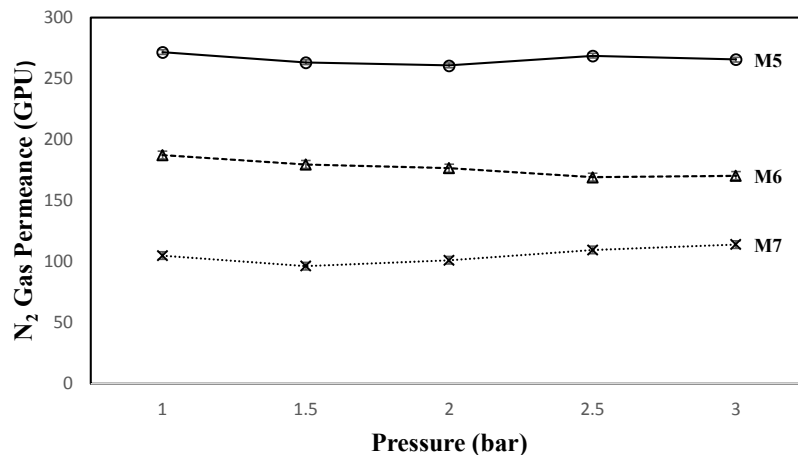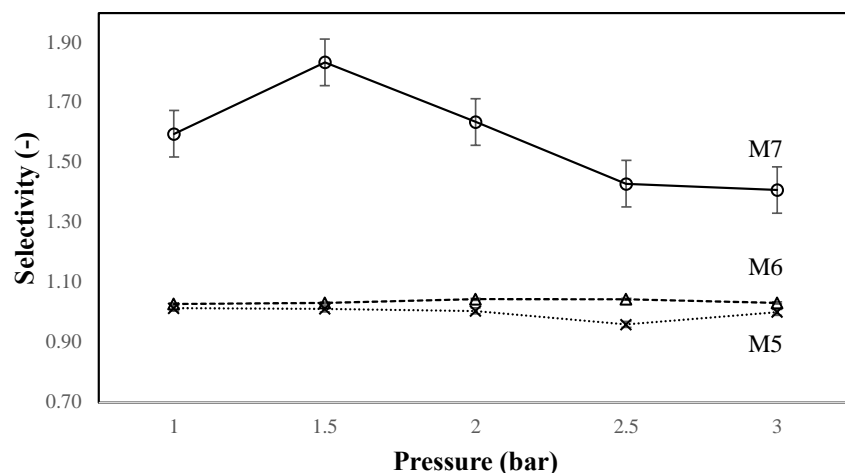

Figure 4 N_2 Permeance for CAB membrane fabricated with different casting thickness of 150 μm (M5), 250 μm (M6), and 300 μm (M7) with solvent evaporation time of 4.5 min, polymer concentration of 4 wt% made up by blending three different molecular weights (Mn) of 12,000, 30,000 and 70,000 at a ratio of 1:2:2, and solvent exchange drying time of 1 hour each for 2-isopropyl alcohol and n-hexane, respectively

3.1.2 Membrane Performance Test

To test the membrane performance, the membranes (M5, M6, and M7) were assessed towards the permeance of CO_2 and N_2, respectively. The results of CO_2 permeance obtained for M5 (150 μm), M6 (250 μm) and M7 (300 μm) at 1 bar to 3 bar were illustrated in

Figure 3. According to Figure 3, the decrease in membrane permeance performance can clearly be visible, where the CO_2 permeance of M5 is the highest at 265.921 ± 2.902 GPU as compared to M6 (179.811 ± 4.229 GPU) and M7 (165.628 ± 3.399 GPU). From the results, it can be concluded

Figure 5 CO_2/N_2 Selectivity for CAB membrane fabricated with different casting thickness of 150 μm (M5), 250 μm (M6), and 300 μm (M7) with solvent evaporation time of 4.5 min, polymer concentration of 4 wt% made up by blending three different molecular weights (Mn) of 12,000, 30,000 and 70,000 at a ratio of 1:2:2, and solvent exchange drying time of 1 hour each for 2-isopropyl alcohol and n-hexane, respectively
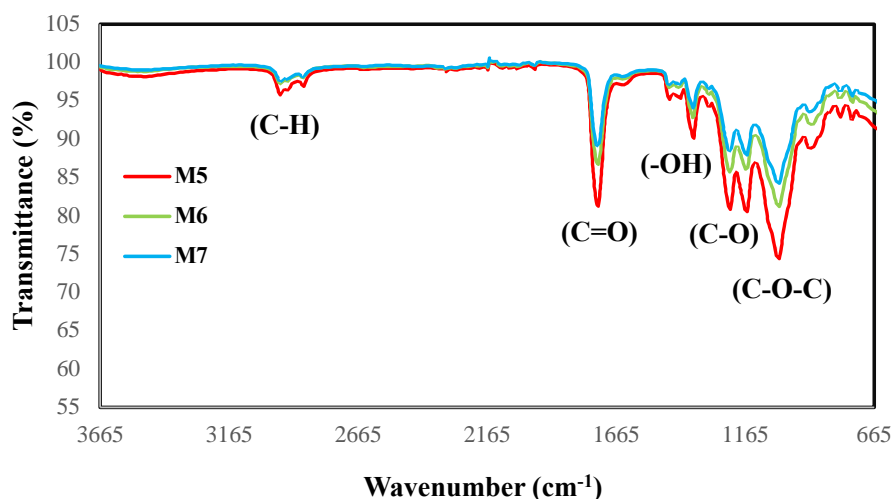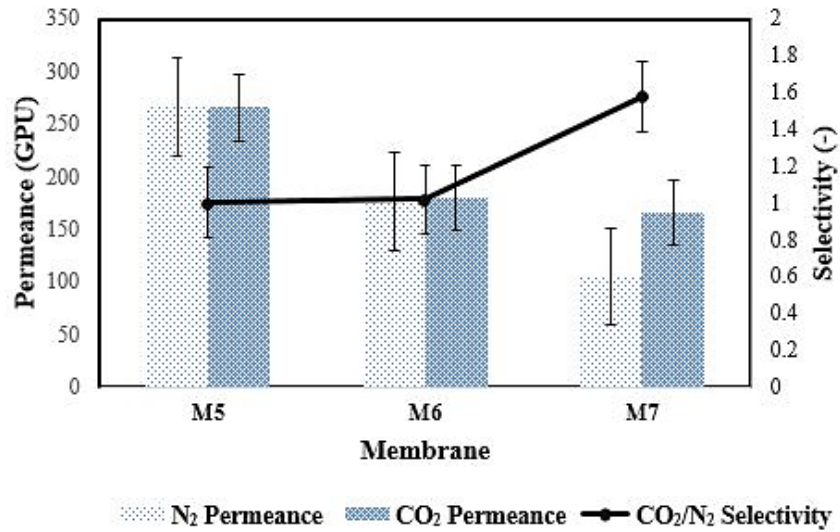

Figure 6 ATR-FTIR spectroscopy for CAB membrane fabricated with different casting thickness of 150 μm (M5), 250 μm (M6), and 300 μm (M7) with solvent evaporation time of 4.5 min, polymer concentration of 4 wt% made up by blending three different molecular weights (Mn) of 12,000, 30,000 and 70,000 at a ratio of 1:2:2, and solvent exchange drying time of 1 hour each for 2-isopropyl alcohol and n-hexane respectively

that the CO_2 permeance increased with the reduction in the casting thickness of the CAB membrane. This is because the skin layer (selective layer) of the membrane decreases as the casting thickness decreases [5]. Hence, the permeance of the membrane increases with a thin membrane because the CO_2 molecules are absorbed at a high level on the skin layer surface and then diffuse through the dense layer of the membrane [20]. Therefore, the best casting thickness was 150 μm (M5)

Figure 7 CO_2 and N_2 Permeance (Left) and Selectivity of CO_2/N_2 (right) for CAB membrane fabricated with fabricated with different casting thickness of 150 μm (M5), 250 μm (M6), and 300 μm (M7) with solvent evaporation time of 4.5 min, polymer concentration of 4 wt% made up by blending three different molecular weights (Mn) of 12,000, 30,000 and 70,000 at a ratio of 1:2:2, and solvent exchange drying time of 1 hour each for 2-isopropyl alcohol and n-hexane, respectively

with a CO_2 permeance of 265.921 ± 2.902 GPU.

Meanwhile, the results of N_2 permeance obtained for M5 (150 μm), M6 (250 μm) and M7 (300 μm) at 1 bar to 3 bar is shown in Figure 4. The results depicted in Figure 4 exhibits a similar trend to the results shown in Figure 3 where the increase in membrane permeance performance can clearly be visible as the casting thickness decreases. The membrane M5 (150 μm) has the highest N_2 permeance at 266.092 ± 1.923 GPU as compared to M6 (250 μm) of 176.413 ± 3.067 GPU and M7 (300 μm) of 105.290 ± 3.095 GPU. The high N_2 permeance of the M5 membrane was due to its thinner membrane thickness of 4.852 ± 0.654 μm as exhibited in Figure 2 (b). This is due to the improvement in the gas permeance of a membrane when the dense skin layer decreases [20]. This is further supported with studies carried out by Jawad *et al.* (2015) who concluded that

a membrane with a thin layer accomplish a high efficiency [6]. In overall, the best casting thickness was 150 μm (M5) with a N_2 permeance of 266.092 ± 1.923 GPU.

Subsequently, the CO_2/N_2 selectivity of the CAB membrane fabricated at different casting thickness of M5 (150 μm), M6 (250 μm), and M7 (300 μm) at 1 bar to 3 bar were studied. From Figure 5, it can be observed that the CO_2/N_2 selectivity increases from 0.9994 ± 0.0099 (M5) to 1.5819 ± 0.0775 (M7). This was due to the thickness of the selective layer of M7 which increased as the casting thickness increased, selectively allowing a specific measure of CO_2 to diffuse through the thick membrane, assisted by the solution-diffusion mechanism [21]. Besides that, the higher selectivity of M7 was also the result of higher carbonyl (C=O) and hydroxyl (O-H) groups stretching vibrations, as shown in Figure 6. According to Shan *et al.* [12], both

C=O and O-H groups are the highly polar functional groups that can affect the gas separation performance. Hence, in this case, these increased polar functional groups (C=O and O-H) interact with the non-polar CO_2, improving the membranes (M3) CO_2/N_2 selectivity [22].

In summary, the overall separation performance of the CAB membrane based on the effect of casting thickness was shown in Figure 7. Based on Figure 7, membrane M6 (250 μm) was preferable due to its better CO_2 permeance of 179.811 ± 4.229 GPU and CO_2/N_2 selectivity of 1.0189 ± 0.0074. This results supports the findings of Firpo *et al*. [7] who concluded that that the permeance shows a strong decrease with increase in thickness but the selectivity does not change significantly in its value.

3.2 Effect of Solvent Evaporation Time

3.2.1 Membrane Characterization

SEM analysis had been carried out to study the membrane morphology and membrane thickness at different evaporation time. Figure 8 illustrates the surface morphology and cross-sectional thickness for the cellulose acetate butyrate (CAB) membranes fabricated at different solvent evaporation time of 3.5 min (M1), 4 min (M2), 4.5 min (M3) and 5 min (M4), respectively. According to Figure 8 (a, c, e and g), the membrane surface remains rough across all solvent evaporation time. The rough surface was due to the hydrophobicity of the membrane surface which reduced the ability of hydrogen bonding formation with water that manipulated the surface morphology [23]. On the other hand, the solvent evaporation time affected the number of nodules on the membrane. With the increase in solvent evaporation time, the nodule distribution on the top surface also increases which is clearly visible from Figure 8 (a, c, e and g). When the membrane formation system loses the solvent environment, chain segments would lose mobility and cannot further adjust their configurations. The loss of solvent environment is too fast during the formation process of the M1 (3.5 min) membrane, and the nodule aggregation would stop at an intermediate stage. But for the formation process of the M4 (5 min) membrane, out-diffusion of solvent is slow enough. Therefore, due to the presence of the solvent atmosphere, the nodular structures can aggregate to form more structures [18].

Furthermore, based on Figure 8 (b, d, f and h), when the solvent evaporation time increased from 3.5 min (M1) to 5 min (M4), the membrane thickness increased from 7.168 ± 1.083 μm to 18.489 ± 1.820 μm. This is because a longer evaporation time would form a less compact polymer region at the top of the casting membrane due to the evaporation of highly volatile solvent [24]. Hence, a longer evaporation time would consequently lead to the formation of an asymmetric membrane with a denser and thicker skin layer [25]. Additionally, the thickness of membrane M2 (4 min) also increased to 20.896 ± 3.432 μm which is similar to M4 (18.489 ± 1.820 μm). Meanwhile, the membrane fabricated at a solvent evaporation time of 4.5 min (M3) showed a thinner membrane of 8.995 ± 1.083 μm compared to M2 and M4. This phenomena can be explained by the compact characteristics of the CAB chains in the formation of the M3 membrane during the controlled solvent evaporation period (4.5 min), forming a thin membrane [2].
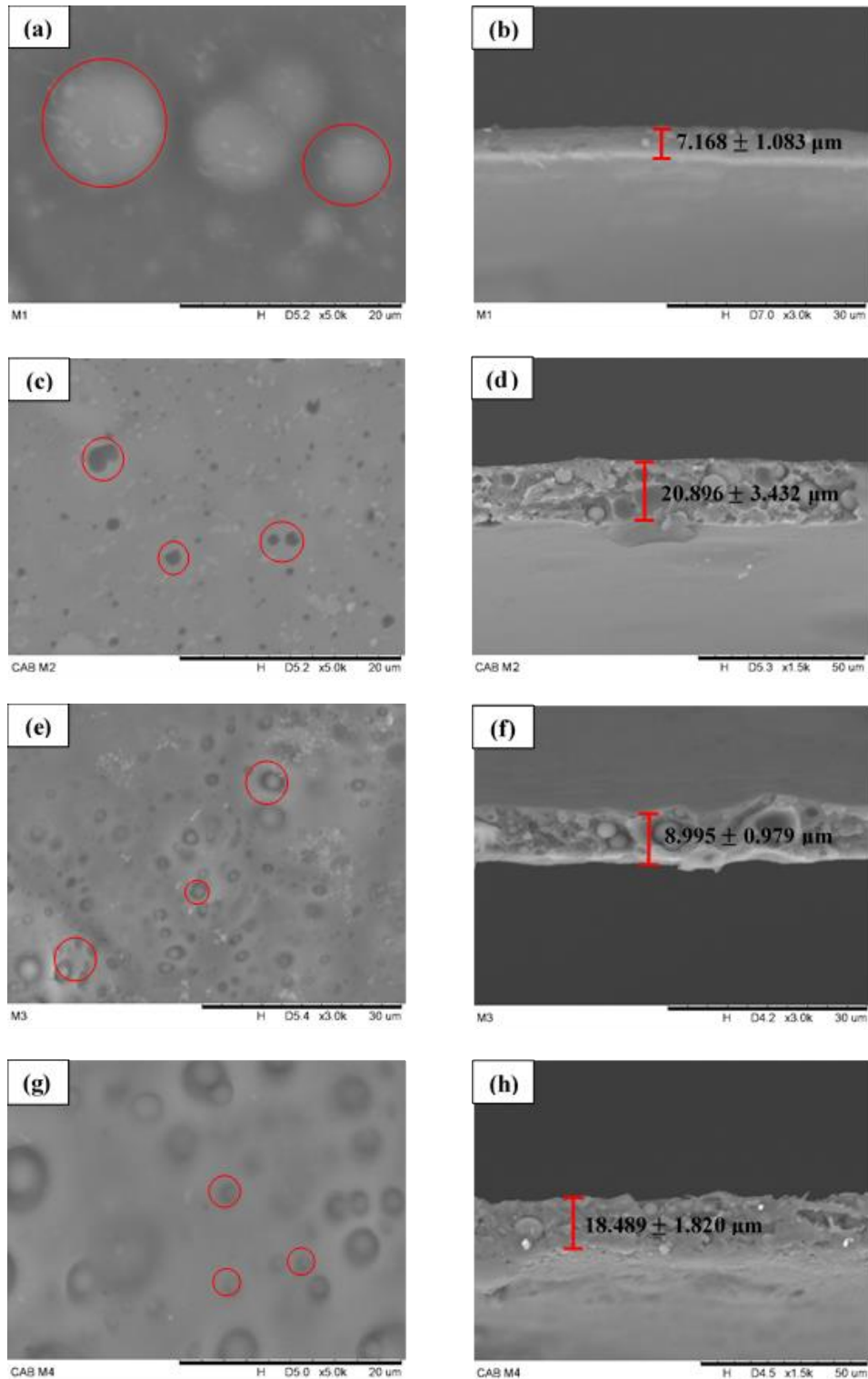
Figure 8 SEM micrographs of membrane surface (left) and cross-section (right) structure synthesized by using 4 wt% of CAB Polymer concentration made up by blending three different molecular weights (Mn) of 12,000, 30,000 and 70,000 at a ratio of 1:2:2, casting thickness of 250 μm, and solvent exchange drying time of 1 hour for 2-isopropyl alcohol and n-hexane each, with different solvent evaporation time of (a-b) 3.5 min (M1), (c-d) 4 min (M2), (e-f) 4.5 min (M3) and (g-h) 5 min (M4)

Based on Figure 9, the membranes (M1, M2, M3 and M4) were tested by the ATR-FTIR spectroscopy to investigate the solvent evaporation
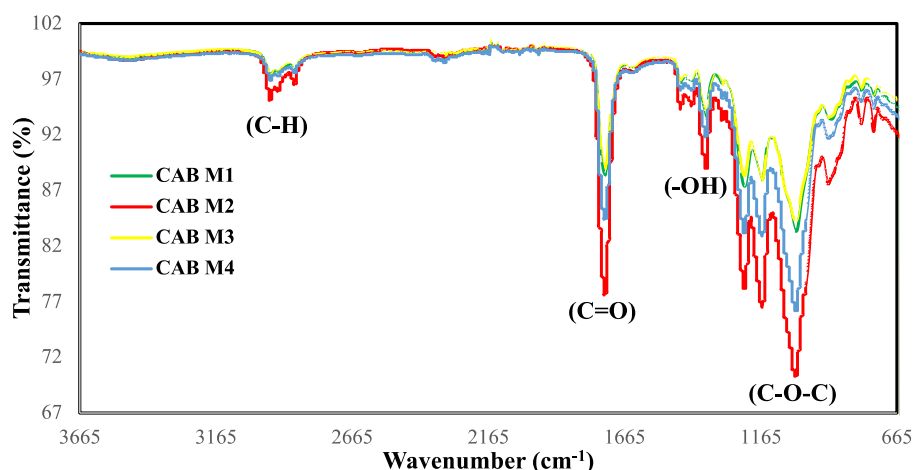
Figure 9 ATR-FTIR spectroscopy for CAB membrane fabricated with different solvent evaporation time of 3.5 min (M1), 4 min (M2), 4.5 min (M3) and 5 min (M4) with casting thickness of 250 μm, polymer concentration of 4 wt% made up by blending three different molecular weights (Mn) of 12,000, 30,000 and 70,000 at a ratio of 1:2:2, and solvent exchange drying time of 1 hour each for 2-isopropyl alcohol and n-hexane, respectively

times on the functional groups of the CAB membrane. The transmittance peak at approximately 2965 cm^{-1} is attributed by C-H stretching [26]. Meanwhile, the peak at around 1736 cm^{-1} is assigned to the carbonyl group vibration of carboxylic acid (C=O) groups, and the peak at 1159 cm^{-1} represents the stretching of acrylate groups (acrylic C-O bond) [27]. Further, the peak at 1038 cm^{-1} is referred to as the C-O-C stretching [28]. In addition, the peak at 1366 cm^{-1} is contributed by the (–OH) group [22].

3.2.2 Membrane Performance Test

Membranes fabricated at a different solvent evaporation time of 3.5 min (M1), 4 min (M2), 4.5 min (M3), and 5 min (M4) were evaluated towards CO_2 permeance by performing a single gas permeation test of CO_2, as exhibited in Figure 10. Based on Figure 10, the CO_2 permeance of M4 is the highest at 191.595 ± 3.197 GPU as compared to M3 (179.811 ± 4.229 GPU), M2 (80.973 ± 3.198 GPU) and M1 (59.698

± 2.204 GPU). This is due to the increase in solvent evaporation time during membrane fabrication which contributed to the increase of the CO_2 permeance. With longer solvent evaporation duration, CAB polymer chains tend to rigidified with higher free volume and thus, improve the penetration of gasses through the resultant membrane [29]. However, the membrane M4 has a poor mechanical strength as the maximum withstanding pressure of M4 was only 2 bar. This could be due to the prolonged solvent-water exchange which deformed the membrane structure, resulting in a reduced mechanical strength of the synthesized membrane [19]. Based on these results, the best solvent evaporation time was 4.5 min (M3) with a CO_2 permeance of 179.811 ± 4.229 GPU.

Next, the membranes fabricated at a different solvent evaporation time of 3.5 min (M1), 4 min (M2), 4.5 min (M3), and 5 min (M4) were tested towards N_2 permeance by performing a single gas permeation test of N_2 as
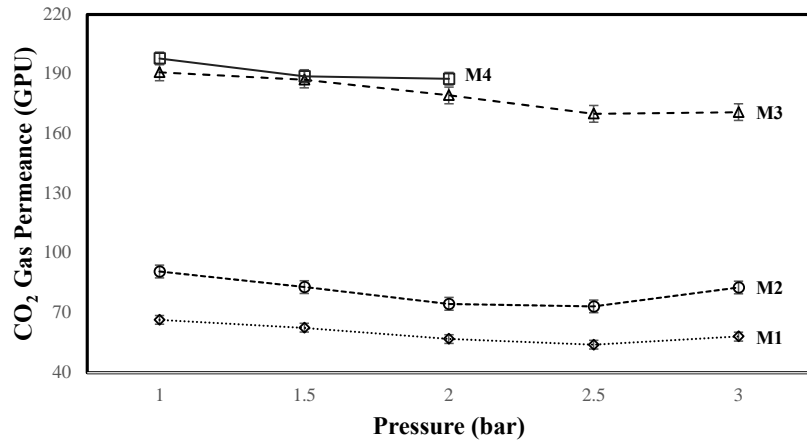
Figure 10 CO_2 Permeance for CAB membrane fabricated with different solvent evaporation time of 3.5 min (M1), 4 min (M2), 4.5 min (M3) and 5 min (M4) with casting thickness of 250 μm, polymer concentration of 4 wt% made up by blending three different molecular weights (Mn) of 12,000, 30,000 and 70,000 at a ratio of 1:2:2, and solvent exchange drying time of 1 hour each for 2-isopropyl alcohol and n-hexane, respectively
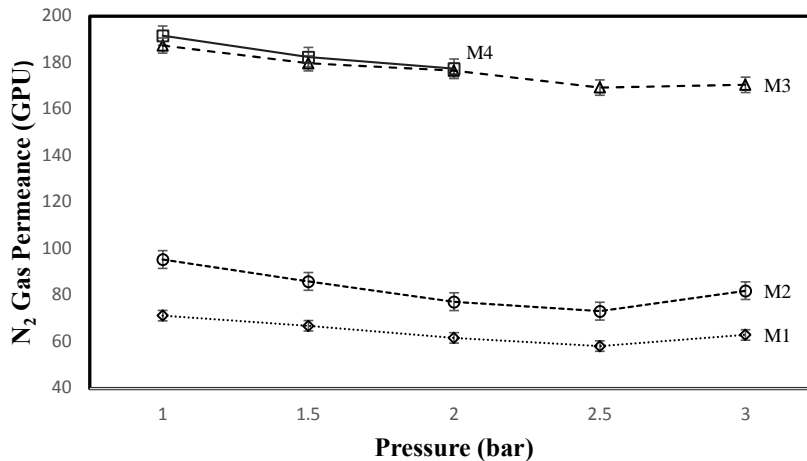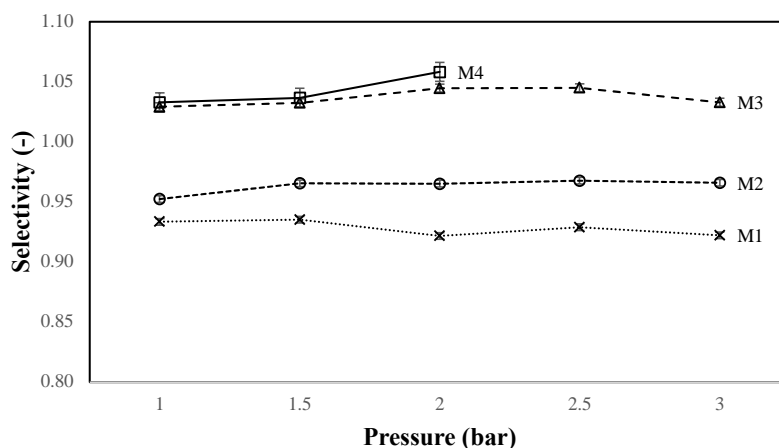

Figure 11 N_2 Permeance for CAB membrane fabricated with different solvent evaporation time of 3.5 min (M1), 4 min (M2), 4.5 min (M3) and 5 min (M4) with casting thickness of 250 μm, polymer concentration of 4 wt% made up by blending three different molecular weights (Mn) of 12,000, 30,000 and 70,000 at a ratio of 1:2:2, and solvent exchange drying time of 1 hour each for 2-isopropyl alcohol and n-hexane, respectively

demonstrated in Figure 11. From Figure 11, it can be seen that the M3 membrane has the highest N_2 permeance of 176.413 ± 3.067 GPU compared to M2 of 82.840 ± 3.817 GPU and M1 of 64.290 ± 2.249 GPU at 1 to 3 bar. The high N_2 permeance of the M3 membrane was due to its thinner membrane thickness of 8.995 ± 1.083 μm as observed in Figure 8 (f) which is ideal for gas separation application as a thinner membrane enforces less flux resistance towards the membrane permeance, resulting in a higher permeance rate [22].

Meanwhile, the CO_2/N_2 selectivity of the CAB membrane fabricated at different solvent evaporation time of M1 (3.5 min), M2 (4 min), M3 (4.5 min) and M4 (5 min) at 1 bar to 3 bar were studied. From Figure 12, it can be observed that the CO_2/N_2 selectivity

Figure 12 CO_2/N_2 Selectivity of CAB membrane fabricated with different solvent evaporation time of 3.5 min (M1), 4 min (M2), 4.5 min (M3) and 5 min (M4) with casting thickness of 250 μm, polymer concentration of 4 wt% made up by blending three different molecular weights (Mn) of 12,000, 30,000 and 70,000 at a ratio of 1:2:2, and solvent exchange drying time of 1 hour each for 2-isopropyl alcohol and n-hexane, respectively
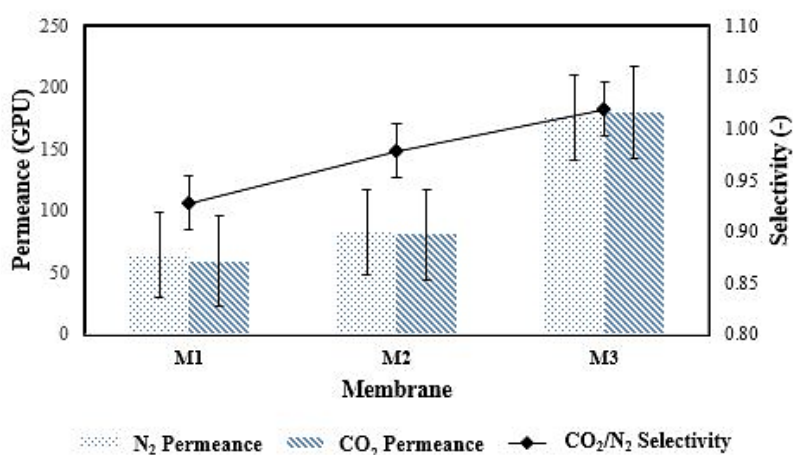
Figure 13 CO_2 and N_2 Permeance (Left) and Selectivity of CO_2/N_2 (right) for CAB membrane fabricated with different solvent evaporation time of 3.5 min (M1), 4 min (M2), and 4.5 min (M3) with casting thickness of 250 μm, polymer concentration of 4 wt% made up by blending three different molecular weights (Mn) of 12,000, 30,000 and 70,000 at a ratio of 1:2:2, and solvent exchange drying time of 1 hour each for 2-isopropyl alcohol and n-hexane, respectively

increased from 0.9283 ± 0.0028 (M1) to 1.0189 ± 0.0074 (M3) as the solvent evaporation duration was increased from 3.5 min (M1) to 4.5 min (M3). This was as a result of higher C=O and –OH group stretching vibrations exhibited by M3 when an ATR-FTIR spectroscopy test was carried out, as shown in Figure 9. According to Shan

et al. (2012), both the carbonyl (C=O) and hydroxyl (O-H) groups are the highly polar functional groups that can affect the gas separation performance [12]. Hence, in this case, these increased polar functional groups (C=O and O-H) interact with the non-polar CO_2, improving the membranes (M3) CO_2/N_2 selectivity [22].

In summary, the overall separation performance of the CAB membrane based on the effect of solvent evaporation time was shown in Figure 13. Based on Figure 13, membrane M3 (4.5 min) has the best CO_2 permeance and CO_2/N_2 selectivity of 179.811 ± 4.229 GPU and 1.0189 ± 0.0074, respectively. This results validates the findings of M. Mubashir *et al.* [29] which demonstrates that an increase in solvent evaporation time would cause the CAB polymer chains to rigidified, enhancing the penetration of gasses through the resultant membrane which would consequently improve the CO_2 permeance of the membrane. In addition to that, an increase in both the C=O and –OH groups stretching vibrations were exhibited by M3 in the ATR-FTIR spectroscopy test (Figure 9). This would improve the interaction between the highly polar functional groups (C=O and –OH) and the non-polar CO_2, improving the CO_2/N_2 selectivity of the membrane [22].

4.0 CONCLUSION

In conclusion, the Cellulose Acetate Butyrate (CAB) membranes with polymer blend of molecular weight (Mn) of 12000, 70000 and 3000 at a ratio of 1:2:2, were successfully fabricated by optimizing the solvent evaporation time and casting thickness of the CAB membrane. The findings of this study validates that the solvent evaporation time influences the membrane morphology and membrane gas separation performance by a great deal. Based on the obtained results, the CO_2/N_2 selectivity was at 1.0189 ± 0.0074 (M3) with a CO_2 and N_2 permeance of 179.811 ± 4.229 GPU and 176.413 ± 3.067 GPU, respectively, when the solvent evaporation time was at 4.5 min. The increase in the duration of the solvent evaporation time caused an increase in the membranes performance due to the strengthened CAB polymer chains with higher free volume.

Moreover, the improvement of the CAB membranes performance was also due to the higher stretching vibration of the polar groups (C=O) and (-OH) available in the membrane structure, which are highly attractive to the non-polar CO_2. In addition to that, the membrane casting thickness is also an essential parameter for membrane fabrication as the properties of the membrane are dependent upon the membrane thickness. When the casting thickness was increased, the CO_2 permeance of the membrane showed a decrease in performance from 265.921 ± 2.902 GPU (M5) (150 μm) to 165.628 ± 3.399 GPU (M7) (300 μm) because of the selective layer of the membrane reduced as the casting thickness decreases. Thus, the permeance of the membrane increases with a thin membrane because the CO_2 molecules are absorbed at a high level on the skin layer surface and then diffuse through the dense layer of the membrane. Hence, the preferable casting thickness was at 250 μm (M6) due to its better CO_2 permeance of 179.811 ± 4.229 GPU and CO_2/N_2 selectivity of 1.0189 ± 0.0074.

REFERENCES

[1] Sreedhar, I., Vaidhiswaran, R., Kamani, B. M., Venugopal, A. 2017. Process and Engineering Trends in Membrane based Carbon Capture. *J. Renew. Sustain Ener.* 68: 659-684.

[2] Lee, R. J., Jawad, Z. A., Ahmad, A. L., Ngo, J. Q., Chua, H. B. 2017. Improvement of CO_2/N_2 Separation Performance by Polymer Matrix Cellulose Acetate Butyrate. *IOP Conference Series: J. Mat. Sci. Eng.* 206: 012072.

[3] IEAGHG. 2014 *Assessment of Emerging CO2 Capture Technologies and Their Potential to Reduce Costs.*

[4] Zhang, Y., Sunarso, J., Liu, S., Wang, R. 2013. Current Status and Development of Membranes for CO_2/CH_4 Separation: A Review. *Int. J. GHG Control.* 12: 84-107.

[5] Ahmad, Olatunji S. Y., Jawad, Z. A. 2017. Thickness Effect on the Morphology and Permeability of CO_2/N_2 Gases in Asymmetric Polyetherimide Membrane. *J. Phys. Sci.* 28: 201-213.

[6] Jawad, Z., A. L. Ahmad, S. C. Low, Zein, S. 2015. Incorporation of Inorganic Carbon Nanotubes Fillers into the Ca Polymeric Matrix for Improvement in Co_2/N_2 Separation. *J. Nanos.* 11: 69-79.

[7] Firpo, G., Angeli, E., Repetto, L., Valbusa, U. 2015. Permeability thickness Dependence of Polydimethylsiloxane (PDMS) Membranes. *J. Membr Sci.* 481: 1-8.

[8] Iqbal, M., Man, Z., Mukhtar, H., Dutta, B. K. 2008. Solvent Effect on Morphology and CO_2/CH_4 Separation Performance of Asymmetric Polycarbonate Membranes. *J. Membr Sci.* 318: 167-175.

[9] Hołda, A. K., Aernouts, B., Saeys, W., Vankelecom, I. F. J. 2013. Study of Polymer Concentration and Evaporation Time as Phase Inversion Parameters for Polysulfone-based SRNF Membranes. *J. Membr Sci.* 442: 196-205.

[10] Haponska, M., Trojanowska, A., Nogalska, A., Jastrzab, R., Gumi, T., Tylkowski, B. 2017. PVDF Membrane Morphology— Influence of Polymer Molecular Weight and Preparation Temperature. *J. Polym.* 9: 718.

[11] Ahmad, A. L., Jawad, Z. A., Low, S. C., Sharif Zein, S. H. 2013. The Functionalization of Beta-cyclodextrins on Multi Walled Carbon Nanotubes: Effects of the Dispersant and Non Aqueous Media. *Current Nanoscience.* 9: 93-102.

[12] Shan, M., Xue, Q., Jing, N., Ling, C., Zhang, T., Yan, Z., Zheng, J. 2012. Influence of Chemical Functionalization on the CO2/N2 Separation Performance of porous Graphene Membranes. *J. Nanoscale.* 4: 5477-5482.

[13] Lee, R. J., Jawad, Z. A., Ahmad, A. L., Chua, H. B. 2018. Incorporation of Functionalized Multi-walled Carbon Nanotubes (MWCNTs) into Cellulose Acetate Butyrate (CAB) Polymeric Matrix to Improve the CO2/N2 Separation. *Process Safety and Environmental Protection.* 117: 159-167.

[14] Lalia, B. S., Kochkodan, V., Hashaikeh, R., Hilal, N. 2013. A Review on Membrane Fabrication: Structure, Properties and Performance Relationship. *J. Desal.* 326: 77-95.

[15] Ye, F., J. M. Zhang, and J. Zhang. 2015. Gas Separation Properties of Cellulose Acetate Butyrate/Mwcnts Mixed Matrix Membranes. *Acta Polymerica Sinica*. 12: 1396-1401.

[16] Khursheed, A. 2007. Scanning Electron Microscope.

[17] Georg Ramer, Lendl., B., 2013. Attenuated Total Reflection Fourier Transform Infrared Spectroscopy. *Encyclopedia of Analytical Chemistry*,

[18] Yiming Zeng, Zhigang Wang, Lijun Wan, Yanqiao Shi, Guanwen Chen, Bai., C. 2003. Surface Morphology and Nodule Formation Mechanism of Cellulose Acetate Membranes by Atomic Force Microscopy. *Institute of Chemistry, Chinese Academy of Sciences, Beijing 100080, People's Republic of China*.

[19] Jawad, Z., A. L. Ahmad, S. C. Low, Zein, S. 2015. Influence of Solvent Exchange Time on Mixed Matrix Membrane Separation Performance for CO2/N2 and a Kinetic Sorption Study. *J. Membr Sci.* 476: 590-601.

[20] Pakizeh, M., Mansoori, S. A. A., Pourafshari Chenar, M., Namvar-Mahboub, M. 2013. Modification of PSf Membrane Nanostructure using Different Fabrication Parameters and Investigation of the CO2 Separation Properties of PDMS-Coated PSf Composite Membranes. *Brazilian J. Chem Eng.* 30: 345-354.

[21] Xing, D. Y., Peng, N., Chung, T.-S. 2010. Formation of Cellulose Acetate Membranes via Phase Inversion Using Ionic Liquid, [BMIM]SCN, As the Solvent. *J. Ind. Eng Chem Res.* 49: 8761-8769.

[22] Lee, R. J., Jawad, Z. A., Ahmad, A. L., Chua, H. B. 2018. Incorporation of Functionalized Multi-walled Carbon Nanotubes (MWCNTs) into Cellulose Acetate Butyrate (CAB) Polymeric Matrix to Improve the CO2/N2 Separation. *J. Process Saf. Environ.* 117: 159-167.

[23] Du, J. R., Peldszus, S., Huck, P. M., Feng, X. 2009. Modification of Poly(vinylidene fluoride) Ultrafiltration Membranes with Poly(vinyl alcohol) for Fouling Control in Drinking Water Treatment. *J. Water Res.* 43: 4559-4568.

[24] Jami'an, H. Hasbullah, F. Mohamed, N. Yusof, N. Ibrahim, Ali, R. R. 2017. Effect of Evaporation Time on Cellulose Acetate Membrane for Gas Separation. *IOP Conference Series: J. Ear. Env. Sci.* 36.

[25] Altun, V., Remigy, J.-C., Vankelecom, I. F. J. 2017. UV-cured Polysulfone-based Membranes: Effect of Co-solvent Addition and Evaporation Process on Membrane Morphology and SRNF Performance. *J. Membr Sci.* 524: 729-737.

[26] Lavorgna, M., Romeo, V., Martone, A., Zarrelli, M., Giordano, M., Buonocore, G. G., Qu, M. Z., Fei, G. X., Xia, H. S. 2013. Silanization and Silica Enrichment of Multiwalled Carbon Nanotubes: Synergistic Effects on The Thermal-mechanical Properties of Epoxy Nanocomposites. *European Poly J.* 49: 428-438.

[27] Suttiwijitpukdee, N., Sato, H., Zhang, J., Hashimoto, T., Ozaki, Y. 2011. Intermolecular Interactions and Crystallization Behaviors of Biodegradable Polymer Blends between Poly

(3-hydroxybutyrate) and Cellulose Acetate Butyrate Studied by DSC, FT-IR, and WAXD. *J. Polym.* 52: 461-471.

[28] Lou, Y., Liu, G., Liu, S., Shen, J., Jin, W. 2014. A Facile Way to Prepare Ceramic-supported Graphene Oxide Composite Membrane via Silane-graft Modification. *J. Appl. Surf. Sci.* 307: 631-637.

[29] M. Mubashir, Y. Y. Fong, C. T. Leng, Keong, L. K. 2018. Enhanced Gases Separation of Cellulose Acetate Membrane Using N-Methyl-1-2 Pyrrolidone as Fabrication Solvent. *Intl. J. A. Mech. Eng.* 15: 4978-4986.